SINGULARITY ANALYSIS OF ANISOTROPIC MULTIMATERIAL CORNERS

A. Barroso, V. Mantič y F. París
School of Engineering, University of Seville
Camino de los Descubrimientos s/n, E-41092 Seville, Spain
e-mail: *abc@esi.us.es, mantic@esi.us.es, paris@esi.us.es*

Abstract

Singular stress states induced at the tip of linear elastic multimaterial corners are characterized in terms of the order of stress singularities and angular variation of stresses and displacements. Linear elastic materials of an arbitrary nature are considered, namely anisotropic, orthotropic, transversely isotropic, isotropic, etc. Thus, in terms of Stroh formalism of anisotropic elasticity, the scope of the present work includes mathematically non-degenerate and degenerate materials. Multimaterial corners composed of materials of different nature are typically present at any metal-composite, or composite-composite adhesive joint. Several works are available in the literature dealing with a singularity analysis of multimaterial corners but involving (in the vast majority) only materials of the same nature (e.g. either isotropic or orthotropic). Although many different corner configurations have been studied in literature, with almost any kind of boundary conditions, there is an obvious lack of a general procedure for the singularity characterization of multimaterial corners without any limitation in the nature of the materials. With the procedure developed here, and implemented in a computer code, multimaterial corners, with no limitation in the nature of the materials and any homogeneous orthogonal boundary conditions, could be analyzed. As a particular case, stress singularity orders in corners involving extraordinary degenerate materials are, to the authors' knowledge, presented for the first time. The present work is based on an original idea by Ting (1997) in which an efficient procedure for a singularity analysis of anisotropic non-degenerate multimaterial corners is introduced by means of the use of a transfer matrix.

1. Introduction

A great deal of research has been carried out in the last few decades regarding the singularity analysis of linear elastic multimaterial corners, producing many useful results available in the literature at present. Nevertheless, the possibility of including any kind of materials in the corner configuration has been to some extent restricted in these works.

Thus, on one hand, multimaterial corners composed exclusively of isotropic materials with almost any kind of boundary conditions were analyzed in a general way by Dempsey & Sinclair (1979, 1981), see also Bogy (1971), Bogy & Wang (1971), Hein & Erdogan (1971).

On the other hand, singularity analysis of multimaterial corners composed exclusively of real anisotropic, but not isotropic, materials was performed, e.g., by Delale (1984), Pageu et al. (1995a, 1996), Ting (1997), Chen (1998). The vast majority of these works, assuming generalized plane strain state or plain stress states, make use of the powerful Lekhnitskii-Eshelby-Stroh complex variable formalism of Anisotropic Elasticity: Lekhnitskii (1938), Eshelby et al. (1953), Stroh (1958, 1962) (in the following referred to as Stroh formalism). Note that in this formalism, isotropic materials are considered as mathematically degenerate materials (Ting, 1996b). This concept refers to repeated complex roots of the characteristic equation with an associated number of linearly independent eigenvectors of the fundamental elasticity matrix **N** smaller than the multiplicity of the repeated complex roots. The structure of the complex variable representations of elastic solutions is different and very cumbersome for mathematically degenerate materials when compared to non-degenerate materials (Ting & Hwu, 1988 and Wang & Ting, 1997). This is the reason why almost all works which apply analytic representations of elastic solutions to perform singularity analysis of anisotropic multimaterial corners include only real anisotropic, monoclinic or orthotropic mathematically non-degenerate materials.

The studies by other authors referenced above are very useful in composite design applications, but of limited application if no isotropic material is allowed to be included together with real anisotropic materials. Very few works, all recent (e.g., Lin and Sung, 1998, Poonsawat et al., 1998, 2001) consider particular cases of bimaterial corners involving degenerate (usually isotropic) as well as non-degenerate (usually orthotropic) materials. Lin and Sung consider degenerate materials (isotropic) by taking the limiting process with the use of L'Hospital rule. Poonsawat et al. present some bimaterial cases with isotropic and orthotropic materials including friction at the interface. Nevertheless, a general procedure for an N-material corner and any material nature, including extraordinary-degenerate materials, is still lacking.

Using a procedure of anisotropic elasticity for non-degenerate materials, it might be possible to overcome the above explained restrictions and to obtain approximate results, if quasi-isotropic materials are applied as described in what follows. Replacing the isotropic material, in the multimaterial corner studied, by an anisotropic material with elastic constants very similar but not exactly equal to those of the isotropic material, the theoretical basis of the procedure (analytical representation of elastic solution) can be used. Thus the results will be as approximate to the exact ones as the values of the anisotropic elastic constants used are close to the real isotropic ones. Nevertheless, numerical problems related to the possible ill-conditioning of the expressions used in this case can be expected to appear. It is important to notice that the mathematical transition from non-degenerate materials (quasi-isotropic) to degenerate ones (isotropic), leads to a non-continuous definition of the matrices of normalized eigenvectors of **N** involved in Stroh formalism. Thus, it is possible to expect lesser accuracy when reaching certain limits in the previously outlined procedure. This kind of procedure can be used if no high accuracy is required. It has to be pointed out that the dependence of the error in the results obtained in this way with respect to the difference of the value of the elastic constants is not easy to estimate.

Numerical tools like the finite element method can also overcome the above difficulties present in the analytical methods, but usually at the expense of a higher computational effort or lesser accuracy if coarse discretizations are used.

The objective of this work is to present and implement in a computer code a general and analytically based procedure to characterize the singular stress field that appears at the tip of an anisotropic linear elastic multimaterial corner, with no limitations on the nature of the material, considering perfect bonding between the materials, and any combination of homogeneous boundary conditions except unilateral friction contact. The Stroh formalism for the degenerate (Ting & Hwu, 1988) cases and extraordinary degenerate (Wang & Ting, 1997) cases of anisotropic materials will be used to this end.

The use of the concept of a transfer matrix in the analysis of multimaterial corners with perfect adhesion between the material wedges (similar to that used in an analysis of a multimaterial infinite strip, see Buffler, 1971) greatly simplifies the procedure, reducing the size of the system considered, see Defourny (1988) in isotropic potential problems, Ting (1997) in anisotropic elasticity and Mantič et al. (2002) in anisotropic potential problems. To take advantage of the concept of the transfer matrix, in the sense of the above mentioned works, the transfer matrix for degenerate materials has been obtained in the present work.

It has to be mentioned that Desmorat (1996) presented another approach for reducing the size of the linear system considered in the case of bimaterial anisotropic elastic corners, based on a suitable pre-elimination of some variables involved. The results of Desmorat's (1996) and Ting's (1997) work can be considered equivalent when free-free bimaterial corners are studied. However, due to the general scope of Ting's (1997) elegant method, based on the transfer matrix concept, this will be the method developed in the present work to analyze anisotropic multimaterial corners involving any kind of linear elastic material, non-degenerate or degenerate.

Following the approach introduced by Mantič et al. (1997), the boundary conditions analyzed in Ting's work (1997), namely free, fixed, and all materials bonded, have been completed by six additional homogeneous boundary conditions in the present work.

It has to be stressed that the theoretical results and the computer code developed in the present work will allow an accurate singularity analysis of metal to composite joints, modelled like multi-material corners with the simultaneous presence of orthotropic (or transversely isotropic) and isotropic materials in the same corner, to be performed. This kind of joint is widely used for example in the aerospace industry.

2. Stroh formalism of anisotropic elasticity

The Stroh formalism (Ting, 1996a) is a powerful approach for solving anisotropic elasticity problems in which a generalized plane strain state: $u_i=u_i(x_1,x_2)$ (i=1,2,3), can be assumed. The Stroh formalism is based on the following eigensystem:

$$\mathbf{N}\boldsymbol{\xi}_\alpha = p_\alpha \boldsymbol{\xi}_\alpha \quad (\alpha = 1,...,6), \tag{1}$$

where p_α and $\boldsymbol{\xi}_\alpha$ are respectively the eigenvalues and eigenvectors of the real fundamental elasticity matrix $\mathbf{N}$ (6×6) defined as follows:

$$\mathbf{N} = \begin{bmatrix} \mathbf{N}_1 & \mathbf{N}_2 \\ \mathbf{N}_3 & \mathbf{N}_1^T \end{bmatrix}, \ \mathbf{N}_1 = -\mathbf{T}^{-1}\mathbf{R}^T, \quad \mathbf{N}_2 = \mathbf{T}^{-1}, \quad \mathbf{N}_3 = \mathbf{R}\mathbf{T}^{-1}\mathbf{R}^{-T} - \mathbf{Q}, \tag{2}$$

Q, **R** and **T** only depend on the elastic constants of the material C_{ijks} ($\sigma_{ij} = C_{ijks}\varepsilon_{ks}$),

$$Q_{ik} = C_{i1k1}, \quad R_{ik} = C_{i1k2} \ \text{ and } \ T_{ik} = C_{i2k2}, \tag{3}$$

and the superscript T denotes the transpose.

The eigenvalues p_α are complex if the strain energy is positive definite, and the eigenvectors $\boldsymbol{\xi}_\alpha^T = \left(\mathbf{a}_\alpha^T, \mathbf{b}_\alpha^T\right)$ have an important physical meaning, with $\mathbf{a}_\alpha$ being proportional to the displacement vector and $\mathbf{b}_\alpha$ being proportional to the traction vector. If p_α and $\boldsymbol{\xi}_\alpha$ satisfy (1), $\bar{p}_\alpha$ and $\bar{\boldsymbol{\xi}}_\alpha$ are also a solution, where the overbar denotes the complex conjugate. Thus, it is habitual to write:

$$\operatorname{Im} p_\alpha > 0, \qquad p_{\alpha+3} = \bar{p}_\alpha, \qquad \boldsymbol{\xi}_{\alpha+3} = \bar{\boldsymbol{\xi}}_\alpha \qquad (\alpha = 1,2,3), \tag{4}$$

with Im standing for the imaginary part.

Equation (1) is only valid when there are three linearly independent eigenvectors ξ_α (α=1,2,3). If the tensor of elastic constants C_{ijks} of a particular material gives rise to an eigensystem with less than three linearly independent eigenvectors ξ_α, the formalism has to be modified (Ting & Hwu, 1988; Wang & Ting, 1997), equations (1) being transformed in the case of two linearly independent eigenvectors to:

$$\mathbf{N}\xi_1 = p_1\xi_1, \ \ \mathbf{N}\xi_2 = p_1\xi_2 + \xi_1, \ \ \mathbf{N}\xi_3 = p_3\xi_3, \quad (p_1 = p_2), \tag{5}$$

and in the case of only one linearly independent eigenvector to:

$$\mathbf{N}\xi_1 = p\xi_1, \ \ \mathbf{N}\xi_2 = p\xi_2 + \xi_1, \ \ \mathbf{N}\xi_3 = p\xi_3 + \xi_2, \quad (p_1 = p_2 = p_3 = p). \tag{6}$$

In this sense, all linear elastic materials can be classified in relation with the character of the eigensystem of **N**, as shown in Table 1 (Ting, 1996b, 1999):

	$p_1 \neq p_2 \neq p_3 \neq p_1$	$p_1 = p_2 \neq p_3$	$p_1 = p_2 = p_3$
3 Linearly Independent Eigenvectors	Simple (SP)	Semisimple (SS)	Extraordinary semisimple (ES) Does not exist
2 Linearly Independent Eigenvectors		Degenerate or non-semisimple (D1)	Degenerate or non-semisimple (D2)
1 Linearly Independent Eigenvectors			Extraordinary degenerate or Extraordinary non-semisimple (ED)

Table 1. Classification of the fundamental elasticity matrix **N**.

Ting (1996b) proved the existence of materials with an ED matrix **N**, as well as the impossibility of finding any material with an ES matrix **N**, unless the strain energy is allowed to be positive semidefinite.

In the following sections, the particular relations satisfied by the eigenvalues p_α and the associate eigenvectors $\xi_\alpha^T = \left(\mathbf{a}_\alpha^T, \mathbf{b}_\alpha^T\right)$ will be used for the three eigensystems (1), (5) and (6). Depending on the number of linearly independent eigenvectors, the following relations apply:

Three linearly independent eigenvectors (**N** is SP or SS).
For (p_α, ξ_α) with α=1,2,3:

$$\left\{\mathbf{Q} + (\mathbf{R} + \mathbf{R}^T)p_\alpha + \mathbf{T}p_\alpha^2\right\}\mathbf{a}_\alpha = 0, \tag{7}$$

$$\mathbf{b}_\alpha = (\mathbf{R}^T + p_\alpha\mathbf{T})\,\mathbf{a}_\alpha = -\frac{1}{p_\alpha}(\mathbf{Q} + p_\alpha\mathbf{R})\mathbf{a}_\alpha .$$

Two linearly independent eigenvectors (**N** is D1 or D2):
For (p_1, ξ_1) and (p_3, ξ_3) equations (7) hold for α=1,3.
For $p_2 = p_1 = p$ and the generalized eigenvector $\xi_2^T = \left(\mathbf{a}_2^T, \mathbf{b}_2^T\right)$:

$$-\left\{\mathbf{Q} + (\mathbf{R} + \mathbf{R}^T)p + \mathbf{T}p^2\right\}\mathbf{a}_2 = \left[2p\mathbf{T} + \mathbf{R} + \mathbf{R}^T\right]\mathbf{a}_1, \tag{8}$$
$$\mathbf{b}_2 = \mathbf{T}\mathbf{a}_1 + \left[\mathbf{R}^T + p\mathbf{T}\right]\mathbf{a}_2 .$$

One linearly independent eigenvector (**N** is ED) with $p_1 = p_2 = p_3 = p$:
For (p_1, ξ_1) equations (7) hold with α=1.
For (p_2, ξ_2) equations (8).
For p_3 and the generalized eigenvector $\xi_3^T = \left(\mathbf{a}_3^T, \mathbf{b}_3^T\right)$:

$$-\left\{\mathbf{Q} + (\mathbf{R} + \mathbf{R}^T)p + \mathbf{T}p^2\right\}\mathbf{a}_3 = \left[2p\mathbf{T} + \mathbf{R} + \mathbf{R}^T\right]\mathbf{a}_2 + \mathbf{T}\mathbf{a}_1, \tag{9}$$
$$\mathbf{b}_3 = \mathbf{T}\mathbf{a}_2 + \left[\mathbf{R}^T + p\mathbf{T}\right]\mathbf{a}_3 .$$

The solution in terms of displacements, $\mathbf{u}$, and the stress function vector, $\boldsymbol{\varphi}$, can be expressed by means of complex (3×3) matrices $\mathbf{A} = \left[\mathbf{a}_1, \mathbf{a}_2, \mathbf{a}_3\right]$ and $\mathbf{B} = \left[\mathbf{b}_1, \mathbf{b}_2, \mathbf{b}_3\right]$ in the following way:

$$\mathbf{u} = \mathbf{A}\mathbf{G} + \overline{\mathbf{A}}\widetilde{\mathbf{G}} , \tag{10}$$
$$\boldsymbol{\varphi} = \mathbf{B}\mathbf{G} + \overline{\mathbf{B}}\widetilde{\mathbf{G}} , \tag{11}$$

where $\mathbf{G}$ can be written in terms of arbitrary functions $f_\alpha(z_\alpha)$ (α=1,2,3) of complex arguments $z_\alpha = x_1 + p_\alpha x_2$, and $\widetilde{\mathbf{G}}$ in terms of $f_{\alpha+3}(\bar{z}_\alpha)$ (α=1,2,3).

For the analysis of stress singularities it is sufficient to take the same function for α=1,2,3, i.e. $f_\alpha(z_\alpha) = f(z_\alpha)\, q_\alpha$ and $f_{\alpha+3}(\bar{z}_\alpha) = f(\bar{z}_\alpha)\, \tilde{q}_\alpha$, where q_α and $\tilde{q}_\alpha$ are arbitrary real or complex constants. Thus, it is possible to write $\mathbf{G} = \mathbf{F}\cdot\mathbf{q}$ and $\widetilde{\mathbf{G}} = \widetilde{\mathbf{F}}\cdot\widetilde{\mathbf{q}}$ with $\mathbf{q} = (q_1, q_2, q_3)^T$ and $\widetilde{\mathbf{q}} = (\tilde{q}_1, \tilde{q}_2, \tilde{q}_3)^T$. The structure of $\mathbf{F}$ (and $\widetilde{\mathbf{F}}$) depends on the number of linearly independent eigenvectors, as shown below, where the prime denotes differentiation with respect to the complex variable *z*.

SP and SS cases (non-degenerate cases):

$$\mathbf{F} = \begin{bmatrix} f(z_1) & 0 & 0 \\ 0 & f(z_2) & 0 \\ 0 & 0 & f(z_3) \end{bmatrix}, \quad \widetilde{\mathbf{F}} = \begin{bmatrix} f(\bar{z}_1) & 0 & 0 \\ 0 & f(\bar{z}_2) & 0 \\ 0 & 0 & f(\bar{z}_3) \end{bmatrix}. \tag{12}$$

D1 and D2 cases (degenerate cases):

$$\mathbf{F} = \begin{bmatrix} f(z_1) & x_2 f'(z_1) & 0 \\ 0 & f(z_1) & 0 \\ 0 & 0 & f(z_3) \end{bmatrix}, \quad \widetilde{\mathbf{F}} = \begin{bmatrix} f(\bar{z}_1) & x_2 f'(\bar{z}_1) & 0 \\ 0 & f(\bar{z}_1) & 0 \\ 0 & 0 & f(\bar{z}_3) \end{bmatrix}, (z_1 = z_2). \tag{13}$$

ED case (extraordinary degenerate case):

$$\mathbf{F}=\begin{bmatrix} f(z) & x_2 f'(z) & \frac{1}{2}x_2^2 f''(z) \\ 0 & f(z) & x_2 f'(z) \\ 0 & 0 & f(z) \end{bmatrix},\ \widetilde{\mathbf{F}}=\begin{bmatrix} f(\bar{z}) & x_2 f'(\bar{z}) & \frac{1}{2}x_2^2 f''(\bar{z}) \\ 0 & f(\bar{z}) & x_2 f'(\bar{z}) \\ 0 & 0 & f(\bar{z}) \end{bmatrix}, (z_1=z_2=z_3=z). \tag{14}$$

In the analysis of singular stress states presented in this work, the function $f(z_\alpha)=z_\alpha^\delta$ will be considered, and therefore

$$f_\alpha(z_\alpha)=z_\alpha^\delta\, q_\alpha\,,\quad f_{\alpha+3}(\bar{z}_\alpha)=\bar{z}_\alpha^\delta\, \tilde{q}_\alpha\,, \tag{15}$$

where δ is the characteristic exponent and, as will be seen, δ-1 defines the order of stress singularity for $0<\delta<1$. If δ is a real number, then $\widetilde{\mathbf{F}}=\overline{\mathbf{F}}$ and $\tilde{q}=\bar{q}$.

The orthogonality and closure relations of the Stroh formalism, which also depend on the number of linearly independent eigenvectors, can be written in the following general form:

$$\mathbf{X}\mathbf{X}^{-1}=\mathbf{X}^{-1}\mathbf{X}=\mathbf{I}, \text{ with: } \mathbf{X}=\begin{bmatrix} \mathbf{A} & \overline{\mathbf{A}} \\ \mathbf{B} & \overline{\mathbf{B}} \end{bmatrix} \text{ and } \mathbf{X}^{-1}=\begin{bmatrix} \mathbf{\Gamma}\mathbf{B}^T & \mathbf{\Gamma}\mathbf{A}^T \\ \mathbf{\Gamma}\overline{\mathbf{B}}^T & \mathbf{\Gamma}\overline{\mathbf{A}}^T \end{bmatrix}, \tag{16}$$

where $\mathbf{I}$ is the identity matrix (6×6), and for the different cases: non-degenerate (SP and SS), degenerate (D1 and D2) and extraordinary degenerate (ED), $\mathbf{\Gamma}$ is expressed as:

$$\underset{\text{SP-SS}}{\mathbf{\Gamma}=\begin{bmatrix} 1 & 0 & 0 \\ 0 & 1 & 0 \\ 0 & 0 & 1 \end{bmatrix}},\quad \underset{\text{D1-D2}}{\mathbf{\Gamma}=\begin{bmatrix} 0 & 1 & 0 \\ 1 & 0 & 0 \\ 0 & 0 & 1 \end{bmatrix}},\quad \underset{\text{ED}}{\mathbf{\Gamma}=\begin{bmatrix} 0 & 0 & 1 \\ 0 & 1 & 0 \\ 1 & 0 & 0 \end{bmatrix}} \tag{17}$$

All linear elastic materials fall inside one of the above mentioned groups (Table 1). Thus, all materials can be studied following the approach of Stroh formalism. Isotropic materials, for example, belong to group D2, with a triple eigenvalue $p=i=\sqrt{-1}$ and two linearly independent eigenvectors.

Following Tanuma (1996), transversely isotropic materials can belong to every group in Table 1, except ED. Transversely isotropic materials can be non-semisimple (D1 or D2), irrespective of the value of their elastic constants in the material coordinate system, with the x_3 axis being perpendicular to the x_1-x_2 tranversely isotropic plane of the material. Simply through the relative position of the material with respect to the coordinate system which defines the generalized plain strain state, the material can be non-degenerate or degenerate, Tanuma (1996).

3. Singularity analysis of anisotropic multimaterial corners including non-degenerate materials

3.1. Summary of Ting's procedure.

The procedure originally developed by Ting (1997) is an efficient tool for the singular characterization of non-degenerate anisotropic multimaterial corners. An N-material corner, with N homogeneous wedges, is represented in Figure 1. The *i-th* material wedge occupies the polar sector $\theta_{i-1} < \theta < \theta_i$, i=1,...,N.

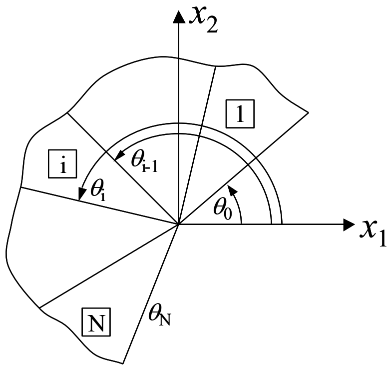

Figure 1. Multimaterial corner.

Perfect bonding is considered between material wedges. Fixed or free boundary conditions are considered at the external faces. The possibility without external faces, all materials being bonded, is also considered and is referred to in this work as a closed corner, as opposed to open corner with external faces.

Consider a polar coordinate system with the origin at the tip of the corner (Figure 1). Then, equations (10) and (11), together with (15), considered for an homogeneous wedge, can be written in the following condensed form, defining the complex variable: $z_\alpha = x_1 + p_\alpha x_2 = r(\cos\theta + p_\alpha \sin\theta) = r\zeta_\alpha(\theta)$:

$$\mathbf{w}(r,\theta) = r^\delta \mathbf{X}\mathbf{Z}^\delta(\theta)\,\mathbf{t}\,, \tag{18}$$

where $\mathbf{X}$ is defined in (16) and $\mathbf{w}(r,\theta)$ is

$$\mathbf{w}(r,\theta) = \begin{bmatrix} \mathbf{u}(r,\theta) \\ \boldsymbol{\varphi}(r,\theta) \end{bmatrix},\ \mathbf{t} = \begin{bmatrix} \mathbf{q} \\ \tilde{\mathbf{q}} \end{bmatrix},\ \mathbf{Z}^\delta(\theta) = \begin{bmatrix} \left\langle \zeta_*^\delta(\theta) \right\rangle & 0 \\ 0 & \left\langle \bar{\zeta}_*^\delta(\theta) \right\rangle \end{bmatrix}. \tag{19}$$

The diagonal matrix $\left\langle \zeta_*^\delta(\theta) \right\rangle = diag\left[\zeta_1^\delta(\theta), \zeta_2^\delta(\theta), \zeta_3^\delta(\theta)\right]$ in $(19)_3$ is associated to matrix $\mathbf{F}$ in $(12)_1$ through the following relation:

$$\mathbf{F} = r^\delta \left\langle \zeta_*^\delta(\theta) \right\rangle \mathbf{q}\,, \tag{20}$$

while $\langle \bar{\zeta}_*^{\delta}(\theta) \rangle = diag\left[\bar{\zeta}_1^{\delta}(\theta), \bar{\zeta}_2^{\delta}(\theta), \bar{\zeta}_3^{\delta}(\theta)\right]$ with $\bar{\zeta}_\alpha^{\delta}(\theta) = (\cos\theta + \bar{p}_\alpha \sin\theta)^{\delta}$, is related to $\widetilde{\mathbf{F}}$ in (12)2 through $\widetilde{\mathbf{F}} = r^{\delta}\langle \bar{\zeta}_*^{\delta}(\theta) \rangle \widetilde{\mathbf{q}}$.

Ting's procedure makes use of a transfer matrix, a matrix which transfers the displacements and stress function vector components from one edge of the material wedge to the other. If equation (18) is evaluated for the *i*-th wedge at $\theta = \theta_{i-1}$ and $\theta = \theta_i$, and $\mathbf{t}$ is eliminated, we obtain:

$$\begin{array}{l} \mathbf{w}(r,\theta_{i-1}) = r^{\delta}\mathbf{X}\mathbf{Z}^{\delta}(\theta_{i-1})\,\mathbf{t}, \\ \mathbf{w}(r,\theta_i) = r^{\delta}\mathbf{X}\mathbf{Z}^{\delta}(\theta_i)\,\mathbf{t}, \end{array} \quad \Rightarrow \quad \mathbf{w}(r,\theta_i) = \mathbf{E}_i\,\mathbf{w}(r,\theta_{i-1}), \tag{21}$$

where, in view of (16),

$$\mathbf{E}_i = \mathbf{X}\mathbf{Z}^{\delta}(\theta_i)\left[\mathbf{Z}^{\delta}(\theta_{i-1})\right]^{-1}\mathbf{X}^{-1}. \tag{22}$$

$\mathbf{E}_i$, called the transfer matrix for the *i*-th wedge, depends on the material properties, on the angles (θ_{i-1} and θ_i) defining the wedge and on the characteristic exponent δ.

Using the continuity conditions introduced by the hypothesis of perfect bonding between the wedges, $\mathbf{w}_i(r,\theta_i) = \mathbf{w}_{i+1}(r,\theta_i)$ $i = (1,\ldots,N-1)$, and the transfer matrix for each wedge, it is easy to arrive at the following expression, which is in fact the expression of the transfer matrix for the whole multimaterial corner, as it relates the variables between its external faces (θ_0 and θ_N):

$$\begin{bmatrix} \mathbf{u}_N(r,\theta_N) \\ \boldsymbol{\varphi}_N(r,\theta_N) \end{bmatrix} = \begin{bmatrix} \mathbf{K}_N^{(1)} & \mathbf{K}_N^{(2)} \\ \mathbf{K}_N^{(3)} & \mathbf{K}_N^{(4)} \end{bmatrix} \begin{bmatrix} \mathbf{u}_1(r,\theta_0) \\ \boldsymbol{\varphi}_1(r,\theta_0) \end{bmatrix}, \text{ or } \mathbf{w}_N(r,\theta_N) = \mathbf{K}_N\mathbf{w}_1(r,\theta_0), \tag{23}$$

where $\mathbf{K}_N$ is obtained by the product of the sequence of the successive transfer matrices $\mathbf{E}_i$ of all the wedges in the corner:

$$\mathbf{K}_N = \mathbf{E}_N \cdot \mathbf{E}_{N-1} \cdot \ldots \mathbf{E}_2 \cdot \mathbf{E}_1. \tag{24}$$

In Ting's work, fixed and free boundary conditions can be prescribed at the external faces of the corner, and the case of all materials being bonded is also considered. The following characteristic equations are obtained from (23) for the different combinations of boundary conditions:

Free-fixed: $\mathbf{u}_N(\theta_N) = \boldsymbol{\varphi}_1(\theta_0) = \mathbf{0}, \quad \Rightarrow \quad \left|\mathbf{K}_N^{(1)}\right| = \mathbf{0}.$ (25)

Fixed - fixed: $\mathbf{u}_N(\theta_N) = \mathbf{u}_1(\theta_0) = \mathbf{0}, \quad \Rightarrow \quad \left|\mathbf{K}_N^{(2)}\right| = \mathbf{0}.$ (26)

Free-free: $\boldsymbol{\varphi}_N(\theta_N) = \boldsymbol{\varphi}_1(\theta_0) = \mathbf{0}, \quad \Rightarrow \quad \left|\mathbf{K}_N^{(3)}\right| = \mathbf{0}.$ (27)

Fixed -free: $\boldsymbol{\varphi}_N(\theta_N) = \mathbf{u}_1(\theta_0) = \mathbf{0}, \quad \Rightarrow \quad \left|\mathbf{K}_N^{(4)}\right| = \mathbf{0}.$ (28)

All bonded: $\boldsymbol{\varphi}_N(\theta_N) = \boldsymbol{\varphi}_1(\theta_0)$ and $\mathbf{u}_N(\theta_N) = \mathbf{u}_1(\theta_0), \Rightarrow \left|\mathbf{K}_N - \mathbf{I}\right| = \mathbf{0}.$ (29)

For open corners the characteristic equations, whose roots δ define the characteristic exponent of the corner problem, are defined as (3×3) determinants (25-28), while in closed corners they are defined as a (6×6) determinant (29). Note that the size of these determinants is independent of the number of materials involved in the corner. The dependence on the wedge materials and wedge geometries is introduced through the evaluation of matrix $\mathbf{K}_N$ in (24).

Two main aspects are worthy of note in Ting's procedure:

- The structure of the procedure allows an implementation in a computer code to be performed in an easy and straightforward way. In the present work it has been carried out using the computer algebra system *Mathematica* (Wolfram, 1991).
- Traditional analytical procedures, without taking advantage of the transfer matrix concept, yield a linear system whose size depends on the number of materials. There are (N-1)×6 equations of continuity at the N-1 interfaces (e.g. at $\theta = \theta_i$: $\mathbf{w}_i(r,\theta_i) = \mathbf{w}_{i+1}(r,\theta_i)$), and 6 equations at the external faces (e.g. fixed-free: $\mathbf{u}(\theta_0) = \mathbf{0}$ and $\boldsymbol{\varphi}(\theta_N) = \mathbf{0}$), making a final linear system of (6N×6N). Ting's procedure directly yields to a linear system whose size is 3×3 or 6×6, see (25-29), irrespective of the number of materials.

In summary, in Ting's procedure, the matrix $\mathbf{K}_N$ (24) is computed by means of the transfer matrices $\mathbf{E}_i$ (22) of each material. For the evaluation of $\mathbf{E}_i$ (22), the matrix $\mathbf{X}$ (16) (and its inverse $\mathbf{X}^{-1}$) are completely defined through **A** and **B**, from Lekhnitskii-Stroh expressions, and the explicit expression of $\mathbf{Z}^\delta(\theta_i)\left[\mathbf{Z}^\delta(\theta_{i-1})\right]^{-1}$ is obtained from Hwu & Ting (1989), see also Ting (1997).

$$\mathbf{Z}^\delta(\theta_i)\left[\mathbf{Z}^\delta(\theta_{i-1})\right]^{-1} = \mathbf{Z}^\delta(\theta_i,\theta_{i-1}) = \begin{bmatrix} \left\langle \zeta_*^\delta(\theta_i,\theta_{i-1}) \right\rangle & \mathbf{0} \\ \mathbf{0} & \left\langle \bar{\zeta}_*^\delta(\theta_i,\theta_{i-1}) \right\rangle \end{bmatrix}, \tag{30}$$

$$\left\langle \zeta_*^\delta(\theta_i,\theta_{i-1}) \right\rangle = diag\{\zeta_1^\delta(\theta_i,\theta_{i-1}), \zeta_2^\delta(\theta_i,\theta_{i-1}), \zeta_3^\delta(\theta_i,\theta_{i-1})\}, \tag{31}$$

$$\zeta_\alpha(\theta_i,\theta_{i-1}) = \frac{\zeta_\alpha(\theta_i)}{\zeta_\alpha(\theta_{i-1})} = \cos(\theta_i - \theta_{i-1}) + p_\alpha(\theta_{i-1})\sin(\theta_i - \theta_{i-1}), \tag{32}$$

$$p_\alpha(\theta_{i-1}) = \frac{p_\alpha \cos(\theta_{i-1}) - \sin(\theta_{i-1})}{p_\alpha \sin(\theta_{i-1}) + \cos(\theta_{i-1})}. \tag{33}$$

3.2 Boundary conditions

The set of boundary conditions in (25-29) can be easily completed to consider any homogeneous orthogonal boundary condition following a procedure introduced by Mantič et al. (1997). Defining θ_a^e for $a = 0,1$ as $\theta_0^e = \theta_0$ and $\theta_1^e = \theta_N$, the unit outward normal and unit tangential vectors ($\mathbf{n}, \mathbf{s}_r, \mathbf{s}_3$, see Figure 2) at θ_0 and θ_N can be written as:

$$\mathbf{n}(\theta_a^e) = (-1)^a\left(\sin\theta_a^e, -\cos\theta_a^e, 0\right),\quad \mathbf{s}_r(\theta_a^e) = (-1)^a\left(\cos\theta_a^e, \sin\theta_a^e, 0\right),\quad \mathbf{s}_3(\theta_a^e) = (0,0,1). \tag{34}$$

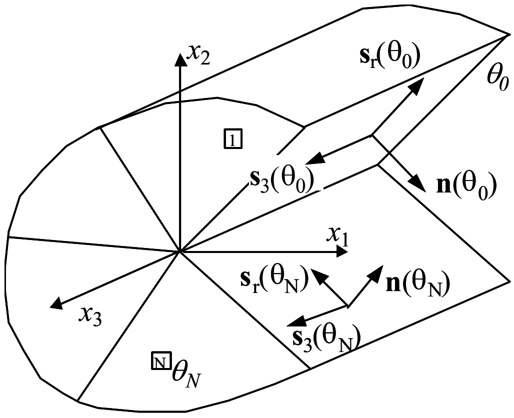

Figure 2. Definition of unit vectors at external faces.

With the above definitions, the usual homogeneous boundary conditions can be expressed through the following compact form (Mantič et al., 1997) for $a = 0, 1$:

$$\mathbf{D}_u(\theta_a^e)\,\mathbf{u}(r,\theta_a^e) + \mathbf{D}_\varphi(\theta_a^e)\,\boldsymbol{\varphi}(r,\theta_a^e) = \mathbf{0}\,, \tag{35}$$

where $\mathbf{D}_u(\theta_a^e)$ and $\mathbf{D}_\varphi(\theta_a^e)$ are real matrices (3×3) which fulfil the following orthogonality conditions:

$$\mathbf{D}_u(\theta_a^e)\mathbf{D}_\varphi^T(\theta_a^e) = \mathbf{D}_\varphi(\theta_a^e)\mathbf{D}_u^T(\theta_a^e) = \mathbf{0}\,. \tag{36}$$

Thus, these boundary conditions, in which the traction vector and the displacement vector are orthogonal to each other, are referred to as orthogonal boundary conditions. Definitions of the above matrices for different boundary conditions are given in Table 2, where **I** and **0** are respectively the unit and zero 3×3 matrices.

Boundary Condition	Matrix Definition	
	$\mathbf{D}_u(\theta_a^e)$	$\mathbf{D}_\varphi(\theta_a^e)$
Free	$\mathbf{0}$	$\mathbf{I}$
Fixed	$\mathbf{I}$	$\mathbf{0}$
Symmetry (only u_θ restricted)	$\left[\mathbf{n}(\theta_a^e),\mathbf{0},\mathbf{0}\right]^T$	$\left[\mathbf{0},\mathbf{s}_r(\theta_a^e),\mathbf{s}_3(\theta_a^e)\right]^T$
Antisymmetry(only u_θ allowed)	$\left[\mathbf{s}_r(\theta_a^e),\mathbf{s}_3(\theta_a^e),\mathbf{0}\right]^T$	$\left[\mathbf{0},\mathbf{0},\mathbf{n}(\theta_a^e)\right]^T$
Only u_r restricted	$\left[\mathbf{s}_r(\theta_a^e),\mathbf{0},\mathbf{0}\right]^T$	$\left[\mathbf{0},\mathbf{n}(\theta_a^e),\mathbf{s}_3(\theta_a^e)\right]^T$
Only u_r allowed	$\left[\mathbf{n}(\theta_a^e),\mathbf{s}_3(\theta_a^e),\mathbf{0}\right]^T$	$\left[\mathbf{0},\mathbf{0},\mathbf{s}_r(\theta_a^e)\right]^T$
Only u_3 restricted	$\left[\mathbf{s}_3(\theta_a^e),\mathbf{0},\mathbf{0}\right]^T$	$\left[\mathbf{0},\mathbf{s}_r(\theta_a^e),\mathbf{n}(\theta_a^e)\right]^T$
Only u_3 allowed	$\left[\mathbf{s}_r(\theta_a^e),\mathbf{n}(\theta_a^e),\mathbf{0}\right]^T$	$\left[\mathbf{0},\mathbf{0},\mathbf{s}_3(\theta_a^e)\right]^T$

Table 2. Boundary condition matrices $\mathbf{D}_u(\theta_a^e)$ and $\mathbf{D}_\varphi(\theta_a^e)$.

Considering the structure of $\mathbf{D}_u(\theta_a^e)$ and $\mathbf{D}_\varphi(\theta_a^e)$ defined in Table 2, the following relation can be verified:

$$\mathbf{D}_u(\theta_a^e)\mathbf{D}_u^T(\theta_a^e) + \mathbf{D}_\varphi(\theta_a^e)\mathbf{D}_\varphi^T(\theta_a^e) = \mathbf{I}\,. \tag{37}$$

Using (36) and (37), it can be shown that the following matrix:

$$\mathbf{D}_{BC}(\theta_a^e) = \begin{bmatrix} \mathbf{D}_u(\theta_a^e) & \mathbf{D}_\varphi(\theta_a^e) \\ \mathbf{D}_\varphi(\theta_a^e) & \mathbf{D}_u(\theta_a^e) \end{bmatrix}, \tag{38}$$

is an orthogonal (6×6) matrix. Thus $\mathbf{D}_{BC}^{-1} = \mathbf{D}_{BC}^T$, and

$$\mathbf{D}_{BC}\mathbf{D}_{BC}^T = \mathbf{I}\,. \tag{39}$$

The subscript BC of matrix $\mathbf{D}_{BC}(\theta_a^e)$ is replaced with the identification of the boundary condition (e.g., $\mathbf{D}_{sym}$ for symmetry or $\mathbf{D}_{free}$ for a free edge).

The boundary conditions have been directly evaluated in terms of the stress function vector, $\boldsymbol{\varphi}$, considering the fact that the traction vector **t** is given by the tangential derivative of $\boldsymbol{\varphi}$, according to the orientation of the tangent vector $\mathbf{s}_r(\theta_a^e)$, as shown in Figure 2. Thus, $t_i = -\dfrac{d\varphi_i}{ds}$. A prescribed zero value of t_i at an edge leads, in view of the fact that the tangential direction coincides at the edge with the radial direction, to: $\dfrac{d\varphi_i}{dr} = 0$.

Considering the structure of the function $\boldsymbol{\varphi}$, see (18-19), which is proportional to r^δ, it is clear that for a particular θ, and excluding the exceptional case $\delta = 0$, the condition $\dfrac{d\varphi_i}{dr} = 0$ is equivalent to $\varphi_i = 0$.

It is easy to show that if the vector $\mathbf{w}(r,\theta)$ is multiplied by the matrix $\mathbf{D}_{BC}$ from the left, the prescribed and the unknown components of $\mathbf{w}(r,\theta)$ appear grouped in two separate blocks. Let us define $\hat{\mathbf{w}}(r,\theta)$ as:

$$\hat{\mathbf{w}}(r,\theta_a^e) = \mathbf{D}_{BC}(\theta_a^e)\,\mathbf{w}(r,\theta_a^e) = \begin{bmatrix} \mathbf{w}_P(r,\theta_a^e) \\ \mathbf{w}_U(r,\theta_a^e) \end{bmatrix}, \tag{40}$$

where $\mathbf{w}_P(r,\theta_a^e)$ and $\mathbf{w}_U(r,\theta_a^e)$ respectively denote vectors of prescribed and unknown components of $\mathbf{w}(r,\theta_a^e)$.

It can be observed that using the definition of $\mathbf{D}_{BC}(\theta_a^e)$ in (38) the prescribed values for $\theta = \theta_a^e$ are those obtained by the expression on the left-hand side in (35). Thus, homogeneous boundary conditions at both θ_a^e can be written as:

$$\mathbf{w}_P(r, \theta_a^e) = 0 . \tag{41}$$

With all the above definitions, equation (23) can be rewritten as:

$$\begin{bmatrix} \mathbf{w}_P(r,\theta_N) \\ \mathbf{w}_U(r,\theta_N) \end{bmatrix} = \begin{bmatrix} \hat{\mathbf{K}}_N^{(1)} & \hat{\mathbf{K}}_N^{(2)} \\ \hat{\mathbf{K}}_N^{(3)} & \hat{\mathbf{K}}_N^{(4)} \end{bmatrix} \begin{bmatrix} \mathbf{w}_P(r,\theta_0) \\ \mathbf{w}_U(r,\theta_0) \end{bmatrix}, \text{ or } \hat{\mathbf{w}}(r,\theta_N) = \hat{\mathbf{K}}_N \, \hat{\mathbf{w}}(r,\theta_0) , \tag{42}$$

where

$$\hat{\mathbf{K}}_N = \mathbf{D}_{BC}(\theta_N) \, \mathbf{K}_N \, \mathbf{D}_{BC}^T(\theta_0) . \tag{43}$$

After applying the homogeneous boundary conditions at $\theta = \theta_a^e$ ($a = 0,1$) in the linear system in (42), the following identity is obtained:

$$\hat{\mathbf{K}}_N^{(2)} \, \mathbf{w}_U(r,\theta_0) = \mathbf{0} . \tag{44}$$

This linear system has a non-trivial solution if and only if the following characteristic equation for δ is fulfilled:

$$\left| \hat{\mathbf{K}}_N^{(2)}(\delta) \right| = \mathbf{0} , \tag{45}$$

where

$$\hat{\mathbf{K}}_N^{(2)} = \mathbf{D}_u(\theta_N)\mathbf{K}_N^{(1)}\mathbf{D}_\varphi^T(\theta_0) + \mathbf{D}_u(\theta_N)\mathbf{K}_N^{(2)}\mathbf{D}_u^T(\theta_0) + \mathbf{D}_\varphi(\theta_N)\mathbf{K}_N^{(3)}\mathbf{D}_\varphi^T(\theta_0) + \mathbf{D}_\varphi(\theta_N)\mathbf{K}_N^{(4)}\mathbf{D}_u^T(\theta_0) . \tag{46}$$

Note that the roots, δ, of the compact expression of the general characteristic equation given by (45) define characteristic exponents for any open multimaterial corner composed of non-degenerate materials with any combination of homogeneous boundary conditions given in Table 2 at both external faces θ_0 and θ_N.

It is easy to verify, using (46) and considering expressions of $\mathbf{D}_u(\theta_a^e)$ and $\mathbf{D}_\varphi(\theta_a^e)$ given in Table 2, that (45) reduces to particular characteristic equations given in (25-28) for the boundary conditions considered there.

4. Transfer matrix for anisotropic degenerate materials (D1 and D2)

In order to take advantage of Ting's approach for singularity analysis of degenerate materials, D1 and D2, see Table 1, it is necessary to deduce the transfer matrix for these materials, analogous to (22). Thus, the modified eigensystem of Stroh formalism (5) has to be used instead of (1).

The generalized eigenvector $\boldsymbol{\xi}_2^T = (\mathbf{a}_2^T, \mathbf{b}_2^T)$ is obtained through (8) instead of (7). The structure of matrix **F** in (13), is not diagonal, and the orthogonality relations change, as shown in (16) and $(17)_2$.

Equation (18) takes the following form now:

$$\mathbf{w}(r,\theta) = r^{\delta}\mathbf{X}\,\mathbf{Z}(\theta,\delta)\,\mathbf{t}\,, \tag{47}$$

where **X** is defined in (16),

$$\mathbf{Z}(\theta,\delta) = \begin{bmatrix} \mathbf{\Psi}(p_*,\theta,\delta) & \mathbf{0} \\ \mathbf{0} & \mathbf{\Psi}(\bar{p}_*,\theta,\delta) \end{bmatrix}, \tag{48}$$

and **t** is defined as in (19). In comparison with (18), the diagonal matrix $\left\langle \zeta_*^{\delta}(\theta) \right\rangle$ associated to matrix **F** in $(12)_1$, is replaced by $\mathbf{\Psi}(p_*,\theta,\delta)$ which is associated to matrix **F** in $(13)_1$ by the following relation:

$$\mathbf{F} = r^{\delta}\mathbf{\Psi}(p_*,\theta,\delta)\,\mathbf{q}\,. \tag{49}$$

Thus, in view of (13) and (49), $\mathbf{\Psi}(p_*,\theta,\delta)$ can be written as:

$$\mathbf{\Psi}(p_*,\theta,\delta) = \begin{bmatrix} \zeta_1^{\delta}(\theta) & \Lambda(p_1,\theta,\delta)\zeta_1^{\delta}(\theta) & 0 \\ 0 & \zeta_1^{\delta}(\theta) & 0 \\ 0 & 0 & \zeta_3^{\delta}(\theta) \end{bmatrix}, \tag{50}$$

$$\text{where: } \Lambda(p_1,\theta,\delta) = \frac{\delta\sin\theta}{\zeta_1(\theta)}, \text{ and } \zeta_\alpha(\theta) = \cos\theta + p_\alpha \sin\theta\,. \tag{51}$$

Evaluating (47) in $\theta = \theta_{i-1}$ and $\theta = \theta_i$, and eliminating vector $\mathbf{t}$, in the same way as shown in Section 3.1, see (21), an expression of the transfer matrix for degenerate materials (D1 and D2) is obtained:

$$\mathbf{E}_i = \mathbf{X}\mathbf{Z}(\theta_i,\delta)\left[\mathbf{Z}(\theta_{i-1},\delta)\right]^{-1}\mathbf{X}^{-1}. \tag{52}$$

The explicit expression of $\mathbf{Z}(\theta_i,\delta)\left[\mathbf{Z}(\theta_{i-1},\delta)\right]^{-1}$ is:

$$\mathbf{Z}(\theta_i,\delta)\left[\mathbf{Z}(\theta_{i-1},\delta)\right]^{-1} = \begin{bmatrix} \mathbf{\Psi}(p_*,\theta_i,\theta_{i-1},\delta) & \mathbf{0} \\ \mathbf{0} & \mathbf{\Psi}(\bar{p}_*,\theta_i,\theta_{i-1},\delta) \end{bmatrix}, \tag{53}$$

with

$$\mathbf{\Psi}(p_*,\theta_i,\theta_{i-1},\delta) = \mathbf{\Psi}(p_*,\theta_i,\delta)\mathbf{\Psi}^{-1}(p_*,\theta_{i-1},\delta)\,, \tag{54}$$

and

$$\mathbf{\Psi}^{-1}(p_*,\theta,\delta)=\begin{bmatrix}\zeta_1^{-\delta}(\theta) & -\Lambda(p_1,\theta,\delta)\zeta_1^{-\delta}(\theta) & 0\\ 0 & \zeta_1^{-\delta}(\theta) & 0\\ 0 & 0 & \zeta_3^{-\delta}(\theta)\end{bmatrix}. \tag{55}$$

Finally, with all the above considerations, the expression of $\mathbf{\Psi}(p_*,\theta_{i-1},\theta_i,\delta)$ is obtained:

$$\mathbf{\Psi}(p_*,\theta_{i-1},\theta_i,\delta)=\begin{bmatrix}\zeta_1^{\delta}(\theta_i,\theta_{i-1}) & K_1\zeta_1^{\delta}(\theta_i,\theta_{i-1}) & 0\\ 0 & \zeta_1^{\delta}(\theta_i,\theta_{i-1}) & 0\\ 0 & 0 & \zeta_3^{\delta}(\theta_i,\theta_{i-1})\end{bmatrix}, \tag{56}$$

where $\zeta_\alpha(\theta_i,\theta_{i-1})$ is defined in (32), and

$$K_1=\frac{\delta\sin(\theta_i-\theta_{i-1})}{\zeta_1(\theta_i)\zeta_1(\theta_{i-1})}. \tag{57}$$

With the above expressions (53-57), the transfer matrix $\mathbf{E}_i$ (52) is now completely defined.

4.1. The particular case of isotropic materials

Isotropic materials belong to group D2 with a triple eigenvalue $p=i=\sqrt{-1}$ and two linearly independent eigenvectors. For these materials all the above expressions simplify, due to the fact that $\zeta_\alpha(\theta)=\cos\theta+i\sin\theta$, which leads to: $|\zeta_\alpha(\theta)|=1$ and $\arg[\zeta_\alpha(\theta)]=\theta$. Thus, $\zeta_\alpha(\theta_i,\theta_{i-1})$ and K_1 (57) can be written as:

$$\zeta_\alpha(\theta_i,\theta_{i-1})=e^{i(\theta_i-\theta_{i-1})},\ \text{and}\ K_1=\frac{\delta\sin(\theta_i-\theta_{i-1})}{e^{i(\theta_i+\theta_{i-1})}}. \tag{58}$$

The expressions of **A** and **B** for isotropic materials are (Ting 1996a):

$$\mathbf{A}=\sqrt{8\mu(1-\nu)}\begin{bmatrix}1 & -\frac{1}{2}i(3-4\nu) & 0\\ i & -\frac{1}{2}(3-4\nu) & 0\\ 0 & 0 & (1-i)\sqrt{2(1-\nu)}\end{bmatrix},\quad \mathbf{B}=\mu\sqrt{8\mu(1-\nu)}\begin{bmatrix}2i & 1 & 0\\ -2 & -i & 0\\ 0 & 0 & (i+1)\sqrt{2(1-\nu)}\end{bmatrix}, \tag{59}$$

where μ and ν are respectively the shear modulus and Poisson's ratio. Substituting (58) in $\mathbf{\Psi}$ (56), together with **A** and **B** in (59), completes the transfer matrix $\mathbf{E}_i$ in (52) for isotropic materials.

5. Transfer matrix for extraordinary degenerate materials (ED)

Using an analogous procedure to that followed in Section 4, the transfer matrix for extraordinary degenerate materials will be deduced in this section.

The eigensystem to be solved in this case is shown in (6). The two generalized eigenvectors $\boldsymbol{\xi}_2^T = (\mathbf{a}_2^T, \mathbf{b}_2^T)$ and $\boldsymbol{\xi}_3^T = (\mathbf{a}_3^T, \mathbf{b}_3^T)$ must satisfy (8) and (9) respectively, while the first eigenvector $\boldsymbol{\xi}_1^T = (\mathbf{a}_1^T, \mathbf{b}_1^T)$ must still satisfy equations (7). The structure of matrix $\mathbf{F}$ is shown in (14) and the orthogonality relations are modified following (16) and $(17)_3$.

Equation (18) for extraordinary degenerate materials, with $p_1 = p_2 = p_3 = p$, can be written as:

$$\mathbf{w}(r,\theta) = r^{\delta} \mathbf{X}\mathbf{Z}(\theta,\delta)\,\mathbf{t}\,. \tag{60}$$

Let us define $\mathbf{Z}(\theta,\delta)$ as in (48):

$$\mathbf{Z}(\theta,\delta) = \begin{bmatrix} \boldsymbol{\Psi}(p,\theta,\delta) & \mathbf{0} \\ \mathbf{0} & \boldsymbol{\Psi}(\bar{p},\theta,\delta) \end{bmatrix}. \tag{61}$$

In comparison with (18), matrix $\left\langle \zeta_*^{\delta}(\theta) \right\rangle$ associated to matrix $\mathbf{F}$ in (12) is replaced by $\boldsymbol{\Psi}(p,\theta,\delta)$, which is associated to matrix $\mathbf{F}$ in (14) by the following relation:

$$\mathbf{F} = r^{\delta} \boldsymbol{\Psi}(p,\theta,\delta)\mathbf{q}\,. \tag{62}$$

Following the same procedure as that presented in Section 4, we can use (14), (62) and the definition of $\Lambda(p_1,\theta,\delta)$ in (51), to finally write $\boldsymbol{\Psi}(p,\theta,\delta)$ as:

$$\boldsymbol{\Psi}(p,\theta,\delta) = \zeta^{\delta}(\theta) \begin{bmatrix} 1 & \Lambda(p,\theta,\delta) & \frac{1}{2}(1-\delta^{-1})\Lambda^2(p,\theta,\delta) \\ 0 & 1 & \Lambda(p,\theta,\delta) \\ 0 & 0 & 1 \end{bmatrix}, \tag{63}$$

where:

$$\Lambda(p,\theta,\delta) = \frac{\delta \sin\theta}{\zeta(\theta)}, \text{ and } \zeta(\theta) = \cos\theta + p\sin\theta \tag{64}$$

The transfer matrix for extraordinary degenerate materials takes the following form:

$$\mathbf{E}_i = \mathbf{X}\mathbf{Z}(\theta_i,\delta)\left[\mathbf{Z}(\theta_{i-1},\delta)\right]^{-1}\mathbf{X}^{-1}, \tag{65}$$

where:

$$\mathbf{Z}(\theta_i,\delta)\left[\mathbf{Z}(\theta_{i-1},\delta)\right]^{-1} = \begin{bmatrix} \boldsymbol{\Psi}(p,\theta_i,\theta_{i-1},\delta) & \mathbf{0} \\ \mathbf{0} & \boldsymbol{\Psi}(\bar{p},\theta_i,\theta_{i-1},\delta) \end{bmatrix}, \tag{66}$$

$$\boldsymbol{\Psi}(p,\theta_i,\theta_{i-1},\delta) = \boldsymbol{\Psi}(p,\theta_i,\delta)\boldsymbol{\Psi}^{-1}(p,\theta_{i-1},\delta)\,, \tag{67}$$

with:

$$\mathbf{\Psi}^{-1}(p,\theta,\delta)=\zeta^{-\delta}(\theta)\begin{bmatrix}1 & -\Lambda(p,\theta,\delta) & \frac{1}{2}(1+\delta^{-1})\,\Lambda^2(p,\theta,\delta)\\ 0 & 1 & -\Lambda(p,\theta,\delta)\\ 0 & 0 & 1\end{bmatrix}. \tag{68}$$

$\mathbf{\Psi}(p,\theta_i,\theta_{i-1},\delta)$ can be written as:

$$\Psi(p,\theta_{i-1},\theta_i,\delta)=\zeta^{\delta}(\theta_i,\theta_{i-1})\begin{bmatrix}1 & K & K\,Z\\ 0 & 1 & K\\ 0 & 0 & 1\end{bmatrix}, \tag{69}$$

where $\zeta(\theta_i,\theta_{i-1})$ is defined as in (32) and K is defined in the same way as in (57):

$$K=\frac{\delta\sin(\theta_i-\theta_{i-1})}{\zeta(\theta_{i-1})\zeta(\theta_i)}, \tag{70}$$

and Z is defined as:

$$Z(p,\theta_{i-1},\theta_i,\delta)=\frac{1}{2}\left(K-\frac{\sin\theta_{i-1}}{\zeta(\theta_{i-1})}-\frac{\sin\theta_i}{\zeta(\theta_i)}\right). \tag{71}$$

With $\mathbf{\Psi}(p,\theta_i,\theta_{i-1},\delta)$ given by (69), the transfer matrix $\mathbf{E}_i$ (65) can then be computed.

6. Singularity analysis of multimaterial corners including any anisotropic material

With the previous results, the transfer matrix can be computed for any wedge material, irrespective of its nature (SP, SS, D1, D2 and ED). A single and robust approach is presented in this section for the singular characterization of any multimaterial corner with perfect adhesion between material wedges and any orthogonal boundary condition or all materials being bonded.

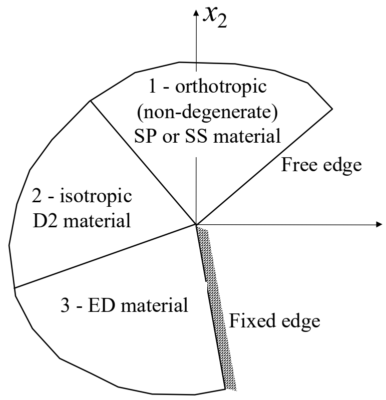

Figure 3. Corner with non-degenerate, degenerate and extraordinary degenerate materials.

Consider, as an example, the three-material corner represented in Figure 3, involving one non-degenerate orthotropic material (SP or SS material), one isotropic material (degenerate material D2) and one extraordinary degenerate material (ED), with free-fixed boundary conditions at the external faces. The singularity analysis of this corner can be performed following steps 1 to 5 described below.

1) Evaluation of the transfer matrix for each material ($\mathbf{E}_i$), using (22) for $\mathbf{E}_1$, (52) for $\mathbf{E}_2$ and (65) for $\mathbf{E}_3$.
2) Evaluation of the corner transfer matrix $\mathbf{K}_3$ (N=3), by the expression in (24), using the matrices $\mathbf{E}_i$ previously obtained in step 1.
3) Application of boundary conditions, using $\mathbf{D}_{free}(\theta_0)$ and $\mathbf{D}_{fixed}(\theta_N)$ (Table 2) to finally obtain the modified corner transfer matrix $\hat{\mathbf{K}}_3$ (43).
4) Evaluation of the determinant of the submatrix $\hat{\mathbf{K}}_3^{(2)}$ of $\hat{\mathbf{K}}_3$, which is explicitly presented in (46). In the case of an open corner, in fact only $\hat{\mathbf{K}}_3^{(2)}$ has to be evaluated, while in the case of closed corners the whole matrix $\hat{\mathbf{K}}_3$ has to be evaluated.
(5) Calculation of roots δ of the characteristic equation (45) (or (29) in the case of closed corners), which represent the characteristic exponents. Roots δ with $0 < \mathrm{Re}(\delta) < 1$ define stress singularity exponents δ-1.

The characteristic equations can be solved using (for example) Muller's (1956) method, when characteristic exponents can be complex. Once the particular value of the characteristic exponent is obtained, the corresponding angular behaviour of displacements and stresses near the tip of the corner can also be computed. The procedure starts with solution of (44) for the δ obtained, then using (40) we obtain $w(r,\theta_0)$. With the transfer matrix of the first material, $w(r,\theta_1)$ can be computed, and in the same way, with each particular transfer matrix, all $w(r,\theta_i)$ i=0,..., N. Once $w(r,\theta_i)$ i=0,..., N are known, the behaviour of stresses and displacements inside each wedge is easy to obtain, using the concept of the transfer matrix between $w(r,\theta_i)$ and $w(r,\theta')$, with $\theta_i < \theta' < \theta_{i+1}$. Stresses are computed by means of: $\sigma_{i1} = -\varphi_{i,2}$ and $\sigma_{i2} = \varphi_{i,1}$.

For closed corners, the linear system to solve is: $(\mathbf{K}_N(\delta) - \mathbf{I})\mathbf{w}(r,\theta_0) = \mathbf{0}$, δ being obtained by means of characteristic equation in (29). Then, using the transfer matrices for each wedge, in just the same way as outlined previously for open corners, displacements and stresses are directly obtained.

7. Numerical examples

7.1. Comparison with previous results obtained by other authors

Several results of singularity analysis of different corner configurations, available in the literature, have been used to study first of all the performance of the computational procedure developed in the present work. Some of them are summarized below.

7.1.1. Isotropic materials (D2 degenerate materials):

Single isotropic wedge: A comparison of the results obtained for a solid sector of an isotropic material of interior angle $\theta_1 - \theta_0 = 280°$, with free-free external faces, versus the results of Seweryn (1994) and Vasilopoulos (1988), is shown in Table 3. The antiplane order of stress singularity is also presented (δ-1=-0.357143). An excellent agreement is achieved in all digits.

Vasilopoulos	Seweryn	Present work
-0.469604280870	-0.469604	-0.469604
	-0.357143	-0.357143
-0.156560431071	-0.156560	-0.156560

Table 3. Results (δ-1) for a single free-free isotropic corner.

Bimaterial isotropic corners: Classical results from Dempsey and Sinclair (1979, 1981) were used. The results obtained for free-free corners (Table 4), and for corners with all materials bonded (Table 5), are all excellent. The mechanical properties of both materials are: E_1=30 GPa, ν_1=0.25, E_2=120 GPa, ν_2=0.31, for results in Table 4 and: E_1=30 GPa, ν_1=0.2, E_2=120 GPa, ν_2=0.3, for results in Table 5. Additional antiplane order of stress singularities are presented in both cases.

	Dempsey & Sinclair	Present work
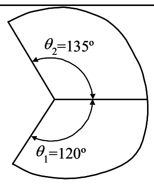	-0.390748	-0.390748
		-0.269076

Table 4. Results (δ-1) for a bimaterial free-free isotropic corner.

	Dempsey & Sinclair	Present work
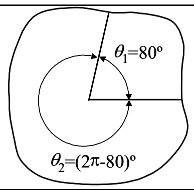	-0.229549	-0.2295490
		-0.1916800
	-0.0742109	-0.0742109

Table 5. Results (δ-1) for a closed bimaterial isotropic corner.

Three-material isotropic corners: Results from Hein & Erdogan (1971) and Pageau et al. (1994) are compared with those obtained in the present work in Tables 6 and 7. The agreement is excellent, including the second case (Table 7), with complex valued order of stress singularities. Additional antiplane order of stress singularities are presented (δ-1=-0.00580724 in Table 6 and δ-1=-0.460283 in Table 7). Mechanical properties for the configuration shown in Table 6 are: E_1=20 GPa, ν_1=0.2, E_2=10 GPa, ν_2=0.2, E_3=0.01 GPa, ν_3=0.2, while in Table 7 E_1=10 GPa, ν_1=0.2, E_2=0.01 GPa, ν_2=0.2, E_3=100 GPa, ν_3=0.2.

	Hein & Erdogan	Pageau et al.	Present work
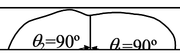			

-0.0226	-0.0226	-0.02263280
		-0.00580724
	-0.0003	-0.00028330

Table 6. Results (δ-1) for a closed three-material isotropic corner with $\theta_1 = \theta_2 = 90^o, \theta_3 = 180^o$.

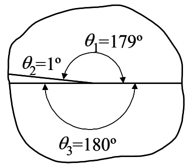

Hein & Erdogan	Pageau et al.:	Present work:
-0.4975±0.1014 *i*	-0.4476±0.0887 *i*	-0.447624±0.088750 *i*
		-0.460273

Table 7. Results (δ-1) for a closed three-material isotropic corner, $\theta_1 = 179^o, \theta_2 = 1^o, \theta_3 = 180^o$.

It has been verified that the singular exponents associated to the antiplane mode in the previous examples agree with those obtained by Mantič et al. (2002) procedure up to six digits or more.

7.1.2. Non-degenerate anisotropic materials:

Bimaterial orthotropic free-free corner: Results from Delale (1984) and Chen (1998) were used in this case. An excellent agreement was found with present results, shown in Table 8. Both materials represent the same orthotropic material equivalent to a fiber reinforced plastic with different orientation of fibers. The fibers are placed in the x_2-x_3 plane, with angles with respect to x_2 axis: ϕ_1=60º and ϕ_2=30º, and the following mechanical properties: E_{11}=163.4 GPa, E_{22}=E_{33}=11.9 GPa, G_{12}=G_{13}=6.5 GPa, G_{23}=3.5 GPa, ν_{12}=ν_{13}=0.3, ν_{23}=0.5.

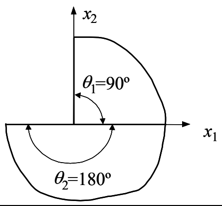

Delale	Chen	Present work
-0.4229	-0.422886	-0.422886
	-0.380828	-0.380828
	-0.047337	-0.047337

Table 8. Results (δ-1) for a free-free bimaterial orthotropic corner.

Interface crack in an orthotropic bimaterial configuration: Results from Wang (1984) and Chen & Huang (1997) were available for this case, in which the agreement with the results obtained by the procedure developed in the present work is also very good. The mechanical properties of the materials are those of a typical graphite-epoxy composite, taking the following values when expressed in orthotropic axes: E_{11}=138 GPa, E_{22}=E_{33}=14.5 GPa, G_{12}=G_{13}=G_{23}=5.9 GPa, ν_{12}=ν_{13}=ν_{23}=0.21. The angle α, see Table 9, is the angle the fiber forms with respect to x_3 axis in the x_1-x_3 plane.

Wang	Chen & Huang	Present work

$\alpha=\pm45^o$	-0.5 -0.5±0.03434 *i*	-0.5 -0.5±0.0343365146 *i*	-0.5 -0.5±0.0343398 *i*
$\alpha=\pm60^o$	-0.5 -0.5±0.02942 *i*	-0.5 -0.5±0.0294152218 *i*	-0.5 -0.5±0.0294132 *i*

Table 9. Results (δ-1) for an interface crack between two orthotropic materials.

Three-material orthotropic corners have also been analyzed, a very good agreement being obtained with available results by Chen (1998) and Pageau et al. (1996).

In view of the excellent agreement obtained between the results of the procedure developed in this work and results of other authors in all studies presented and also others not presented here, for the sake of brevity, the computer code developed here can be considered successfully verified.

7.2. Isotropic-orthotropic bimaterial corner

In every metal to composite or composite to composite adhesive joint, an example of an isotropic-orthotropic bimaterial corner, with the simultaneous presence of non-degenerate and degenerate materials, can be found.

Paying attention to the corner depicted in Figure 4, the procedure presented in this work can be used without any of the limitations that usually appear in traditional approaches which make use of Stroh formalism. In the vast majority of cases, these limitations are due to the fact that isotropic materials as well as any other anisotropic material wich is mathematically degenerate, cannot be included in the analysis.

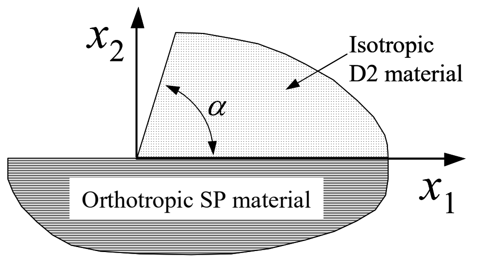

Figure 4. Bimaterial corner with SP and D2 materials.

The materials in the corner (Figure 4), have the following properties:

Composite material (orthotropic non-degenerate, SP material):
E_{11}=141.3 GPa E_{22}=9.58 GPa, E_{33}=9.58 GPa
G_{12}=5.0 GPa, G_{13}=5.0 GPa, G_{23}=3.5 GPa
ν_{12}=0.3, ν_{13}=0.3, ν_{23}=0.32

Epoxy adhesive (isotropic, D2 material):
E=3 GPa, ν=0.3

In Figure 5, the adhesive angle (α) varies from 0º to 180º and the fiber reinforced plastic has the fiber oriented in x_1 direction. Two order of stress singularities are obtained until an angle of approximately α=85º is reached. Starting from this angle, three real order of stress singularities are obtained.

Before the adhesive angle reaches 160º, two real roots convert into two complex conjugate roots. Similar results are obtained for two isotropic and two orthotropic free-free corners. Finally, for the interface crack (α=180º), a real root of 0.5 and two complex conjugate roots with real part equal to 0.5 are obtained.

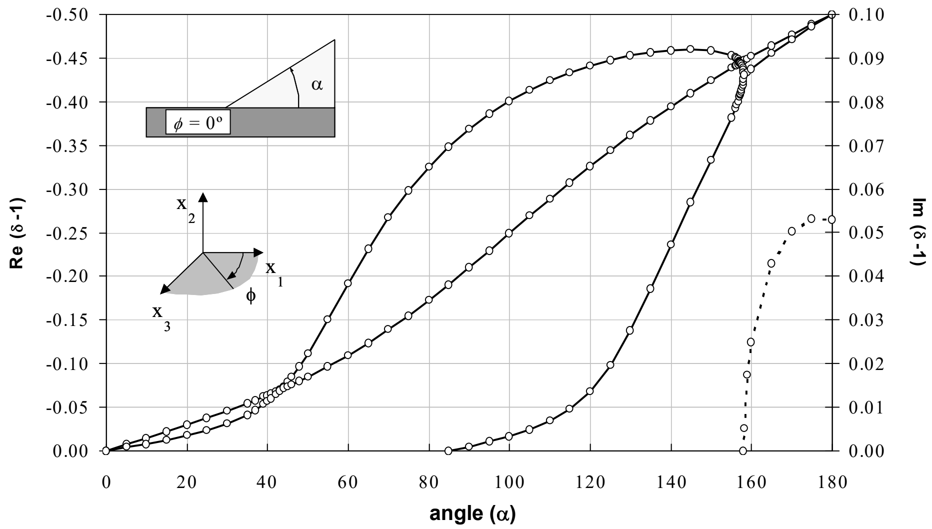

Figure 5. Order of stress singularities (δ-1) for a bi-material SP-D2 corner.

The angular behaviour of displacements u_r, u_θ and the stress components σ_{rr}, $\sigma_{r\theta}$, $\sigma_{\theta\theta}$, calculated using $w(r,\theta)$ and $\sigma_{i1} = -\varphi_{i,2}$, $\sigma_{i2} = \varphi_{i,1}$, are presented in Figure 6, for α=70º for one of the singularity modes with δ-1=-0.266941.

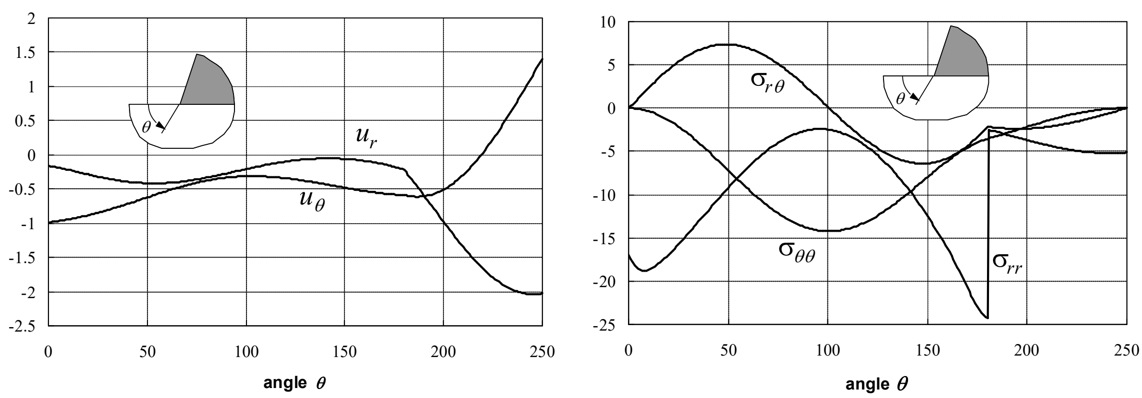

Figure 6. Angular behaviour of displacements and stresses for α=70º and δ-1=-0.266941.

It can be observed that the stress components $\sigma_{r\theta}$ and $\sigma_{\theta\theta}$ fulfil the boundary conditions at the external faces (free-free), and that σ_{rr} is not continuous at the interface between both materials. Displacements are continuous at the interface but not their slope.

7.3. Corners involving extraordinary degenerate (ED) materials

To the authors' knowledge, no results are available for corners involving extraordinary degenerate materials. In fact, these materials have been proved to exist only in recent years (Ting, 1996b).

From Ting (1996b), it is known that a particular group of ED materials can be described with the following reduced elastic compliance matrix:

$$\mathbf{s}' = s'_{11}\begin{bmatrix} 1 & 0 & \gamma & 0 & 0 \\ 0 & \alpha & 0 & 0 & 0 \\ \gamma & 0 & \alpha^{-1} & 0 & 0 \\ 0 & 0 & 0 & 1 & \psi \\ 0 & 0 & 0 & \psi & \alpha(3-\alpha) \end{bmatrix}, \tag{72}$$

where $\psi = \pm(\alpha^{-1}(1-\alpha)^3)^{1/2} - \gamma$, and the following has to be fulfilled: $s'_{11} > 0$, $1 > \alpha > 0$, $\alpha^{-1} > \gamma^2$ and $\alpha(3-\alpha) > \psi^2$. For the numerical example presented in this work, the following values have been taken: $s'_{11} = 1$, $\alpha = \frac{1}{2}$, $\gamma = 1$ and the positive sign in ψ, resulting in:

$$\mathbf{s}' = \begin{bmatrix} 1 & 0 & 1 & 0 & 0 \\ 0 & \frac{1}{2} & 0 & 0 & 0 \\ 1 & 0 & 2 & 0 & 0 \\ 0 & 0 & 0 & 1 & -\frac{1}{2} \\ 0 & 0 & 0 & -\frac{1}{2} & \frac{5}{4} \end{bmatrix}. \tag{73}$$

In Figure 7, the order of stress singularities for a single free-free wedge of the above ED material, from α=180º to the crack configuration, α=360º, is presented.

Two real order of stress singularities are obtained until α=260º, where a third real singularity solution appears. For the crack configuration (α=360º) three real order of stress singularities, with value -0.5, are obtained. The numerical results obtained are presented in Table 10 for some particular values of α.

In Figure 8, a free-free three-material corner involving a 90º wedge of as SP (orthotropic non-degenerate material), a 90º of a D2 (isotropic material) and a 90º of a ED material is presented. The mechanical properties of the orthotropic and isotropic material are the same as used in Section 7.2, while the ED material has the properties given above, in (73).

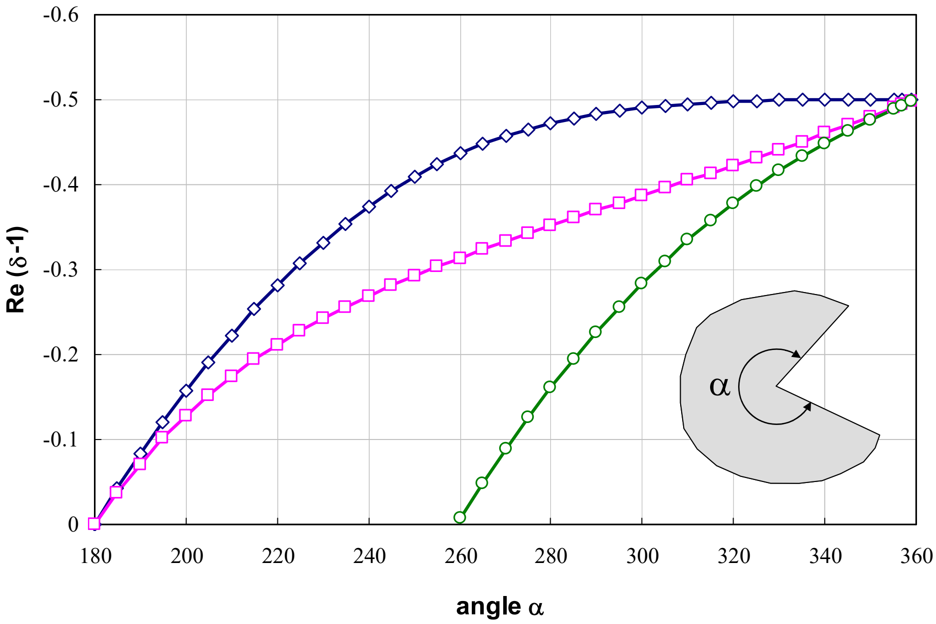

Figure 7. Order of stress singularities (δ-1) for a single free-free ED wedge.

α=200º	-0.15672	-0.128226	
α=240º	-0.374451	-0.269291	
α=280º	-0.472353	-0.351773	-0.161211
α=320º	-0.497632	-0.422641	-0.378599
α=355º	-0.499996	-0.490131	-0.488593

Table 10. Numerical results for some particular cases of Figure 7.

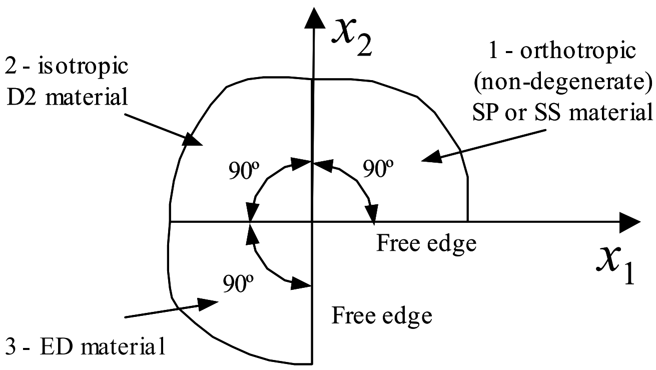

Figure 8. Free-free three-material corner with 90º wedges of SP, D2 and ED materials.

For this particular configuration, a real (δ-1=-0.323997) and two complex conjugate (δ-1=-0.354922±0.152318 i) orders of stress singularity were found.

8. Conclusions

In the present work, a powerful procedure for the singularity analysis of anisotropic multimaterial corners allowing any kind of linear elastic anisotropic material to be considered has been completed and implemented in a computer code.

The transfer matrix for mathematically degenerate materials has been obtained in the framework of Stroh formalism, and explicit expressions have been presented. This allows the original procedure developed by Ting (1997) for the singular characterization of multimaterial anisotropic corners to be completed with the possibility of including degenerate materials in the analysis. As isotropic materials can be considered degenerate materials in Stroh formalism of anisotropic elasticity, the singular analysis is now open to materials of this kind, as well as any other degenerate and extraordinary degenerate material.

A *Mathematica* (Wolfram, 1991) code has been implemented for the calculation of the order of stress singularities, as well as the graphical representation of displacements and stresses. This practical computational tool has shown excellent agreement when comparing with previous results available in the literature, from the single isotropic wedge to the orthotropic three-material corner.

The implemented code has been used to analyze a corner with simultaneous presence of both degenerate (isotropic) and non-degenerate (orthotropic) materials, and also corners involving extraordinary degenerate materials which, to the authors' knowledge, are studied for the first time.

With the computational tool developed, any bidimensional corner configuration can be characterized, considering perfect bonding at interfaces, and any homogeneous orthogonal boundary condition at outer interfaces of the corner (also all bonded). Note that only power type singularities have been considered in this work. The presence of logarithmic singularities can be analyzed using the well-known approach developed by Dempsey and Sinclair (1979), Dempsey (1995), Ting (1996a), Sinclair (1999) and others. The study carried out is a previous step to calculating stress intensity factors (by means, for instance, of the finite element or boundary element methods). The possibility of studying proposals of failure criteria for adhesively bonded joints, based on fracture mechanics, will then be opened up.

9. Acknowledgements

The study has the financial support of the Spanish Ministry of Science and Technology (PROFIT 2001, Project EUREKA Σ!1882) and Ministry of Education and Culture (Projects No. PB98-1118, MAT 2000-1115). The authors gratefully acknowledge helpful information from SACESA.

10. References

Bogy, D.B. Two edge-bonded elastic wedges of different materials and wedges angles under surface tractions. *Journal of Applied Mechanics* 38 (1971) 377-386.

Bogy, D.B. and Wang, K.C. Stress singularities at interface corners in bonded dissimilar isotropic elastic materials. *International Journal of Solids and Structures* 7 (1971) 993-1005.

Buffler, H. Theory of elasticity of a multilayered medium. *Journal of Elasticity* 1 (1971) 125-143.

Chen W.H. and Huang, T.F. Stress singularity of edge delamination in angle-ply and cross-ply laminates. *Journal of Applied Mechanics* 64 (1997) 525-531.

Chen, D.H. and Nisitani, H. Singular stress field near the corner of jointed dissimilar materials. *Journal of Applied Mechanics*. 60 (1993) 607-613.
Chen, H. P. Stress singularities in anisotropic multimaterial wedges and junctions. *International Journal of Solids and Structures* 35 (1998) 1057-1073.
Defourny, M. Singular point theory in Laplace field. C.A. Brebia (ed.), *Boundary Elements X*, Vol. 1, Springer Verlag, Berlin, (1988) 165-180.
Delale, F. Stress singularities in bonded anisotropic materials. *International Journal of Solids and Structures* 20 (1984) 31-40.
Dempsey, J.P. and Sinclair, G.B. On the stress singularities in the plane elasticity of the composite wedge. *Journal of Elasticty* 9 (1979) 373-391.
Dempsey, J.P. and Sinclair, G.B. On the singular behaviour of a bi-material wedge. *Journal of Elasticty* 11 (1981) 317-327.
Dempsey, J.P. Power-logarithmic stress singularities at bimaterial corners and interface cracks. *Journal of Adhesion Science and Technology* 9 (1995) 253-265.
Desmorat, R. Champs singuliers dans un bi-matériau en élasticité plane anisotrope. C.R. Acad. Sci. Paris, t.322, Série IIb, (1996) 355-362.
Eshelby, J.D., Read, W.T. and Shockley, W. Anisotropic elasticity with applications to dislocation theory. *Acta Metallurgica* 1 (1953) 251-259.
Hein, V.L. and Erdogan, F. Stress singularities in a two-material wedge. *International Journal of Fracture Mechanics* 7 (1971) 317-330.
Hwu, C. & Ting, T.C.T. Two-dimensional problems of the anisotropic elastic solid with an elliptic inclusion. *Quarterly Journal of Mechanics and Applied Mathematics* 42 (1989) 553-572.
Lekhnitskii, S.G. Some cases of the elastic equilibrium of a homogeneous cylinder with arbitrary anisotropy", *Applied Mathematics and Mechanics* (in Russian) 2 (1938) 345-367.
Lin, Y.Y. and Sung, J.C. Stress singularities at the apex of a dissimilar anisotropic wedge. *Journal of Applied Mechanics* 65 (1998) 454-463.
Mantič, V., París, F. and Berger, J. Singularities in 2D anisotropic potential problems in multi-material corners. Real variable approach. *submitted for publication* (2002).
Mantič, V., París, F. and Cañas, J. Stress singularities in 2D orthotropic corners. *International Journal of Fracture* 83 (1997) 67-90.
Muller, D.E. A method for solving algebraic equations using an automatic computer. *Mathematical Tables and Computations* 10 (1956) 208-215.
Pageau, S.S. Joseph, P.F. and Biggers, Jr., S.B. The order of stress singularities for bonded and disbonded three-material junctions. *International Journal of Solids and Structures* 31 (1994) 2979-2997.
Pageau, S.S., Joseph, P.F. and Biggers, Jr., S.B. Finite element evaluation of free-edge singular stress fields in anisotropic materials. *International Journal for Numerical Methods in Engineering* 38 (1995a) 2225-2239.
Pageau, S.S., Joseph, P.F. and Biggers, Jr., S.B. Singular antiplane stress fields for bonded and disbonded three-material junctions. *Engineering Fracture Mechanics* 52 (1995b) 821-832.
Pageau, S.S. and Biggers, Jr., S.B. A finite element approach to three-dimensional singular stress states in anisotropic multimaterial wedges and junctions. *International Journal of Solids and Structures* 33 (1996) 33-47.
Poonsawat, P., Wijeyewickrema, A.C. and Karasudhi, P. Singular stress fields of an anisotropic composite wedge with a frictional interface. ASCE 12th Engineering Mechanics Conference, La Jolla, San Diego, CA (1998) 578-581.
Poonsawat, P., Wijeyewickrema, A.C. and Karasudhi, P. Singular stress fields of angle-ply and monoclinic bimaterial wedges. *International Journal of Solids and Structures* 38 (2001) 91-113.
Seweryn, A. Brittle fracture criterion for structures with sharp notches. *Engineering Fracture Mechanics* 47 (1994) 673-681.
Sinclair, G.B. Logarithmic stress singularities resulting from various boundary conditions in angular corners of plates in extension. *ASME Journal of Applied Mechanics* 66 (1999) 556-560.
Stroh, A.N. Dislocations and cracks in anisotropic elasticity", *Philosophical Magazine* 3 (1958) 625-646.
Stroh, A.N. Steady state problems in anisotropic elasticity. *Journal of Mathematics and Physics* 41 (1962) 77-103.
Tanuma, K. Surface-impedance tensors of transversely isotropic elastic materials. *Quarterly Journal of Mechanics and Applied Mathematics* 49 (1996) 29-48.

Ting, T.C.T. and Hwu, C. Sextic formalism in anisotropic elasticity for almost non-semisimple matrix N. *International Journal of Solids and Structures* 24 (1988) 65-76.
Ting, T.C.T. *Anisotropic Elasticity: Theory and Applications*. Oxford University Press (1996a).
Ting, T.C.T. Existence of an extraordinary degenerate matrix N for anisotropic elastic materials. *Quarterly Journal of Mechanics and Applied Mathematics* 49 (1996b) 405-417.
Ting, T.C.T. Stress singularities at the tip of interfaces in polycrystals. *Damage and Failure of Interfaces*, Rossmanith (ed.) Balkema, Rotterdam (1997) 75-82.
Ting, T.C.T. A modified Lekhnitskii formalism à la Stroh for anisotropic elasticity and classifications of the 6×6 matrix N. *Proceedings of the Royal Society of London* A 455 (1999) 69-89.
Vasilopoulos, D. On the determination of higher order terms of singular elastic stress fields near corners. *Numerische Mathematik* 53 (1988) 51-95.
Wang Y.M. and Ting, T.C.T. The Stroh formalism for anisotropic materials that possess an almost extraordinary degenerate matrix N. *International Journal of Solids and Structures* 34 (1997) 65-76.
Wang, S.S. Edge delamination in angle-ply composite laminates. *AIAA Journal* 22 (1984) 256-264.
Wolfram, S. *Mathematica, A system for doing mathematics by computer*. Addison-Wesley, Redwood City (1991).